Submission code: YQNV7X6KQJ

See this and other abstracts on our website: https://home.sbgf.org.br/Pages/resumos.php

Shear velocity inversion using hydrophone data in the Brazilian pre-salt

Renan Sales (Tecgraf Institute/PUC-Rio), Francisco Neto (Tecgraf Institute/PUC-Rio), Deane Roehl (Tecgraf Institute/PUC-Rio), Jorge Lopez (Shell Brasil Petroleo)

Shear velocity inversion using hydrophone data in the Brazilian pre-salt

Abstract

The pressure wavefield remains the primary product in the seismic acquisition industry due to the maturity of modeling and processing techniques. However, emerging exploration targets—such as deep and thin pre-salt reservoirs—require higher modeling accuracy due to the shorter wavelengths involved. Elastic modelling offers the means to capture short wavelengths by incorporating S-waves, which are more sensitive to subsurface heterogeneities. However, a key challenge in elastic modeling lies in constructing an accurate shear wave velocity model, which is essential for elastic wave propagation. This study demonstrates the feasibility of recovering the shear wave velocity model using elastic full waveform inversion (FWI) applied to pressure seismograms (hydrophone recordings). The proposed strategy was applied to a conceptual model based on the Brazilian pre-salt, showing promising results for enhancing subsurface characterization in complex geological settings.

Introduction

Full-waveform inversion is widely recognized as one of the most effective techniques for deriving accurate subsurface property models from seismic data (Virieux and Operto, 2009). However, this inversion is computationally intensive in processing and memory usage. Those drawbacks are even more evident for shear wave velocity inversion, where the low velocities require finer spatial and temporal discretization. In addition, the shear wave velocity model may have some anomalies associated with crosstalk events and strong numerical artifacts (Sears et al., 2008).

Shear velocity models are often estimated using multicomponent inversion approaches. For example, Cho et al. (2022) utilize the horizontal geophone components to retrieve the shear wave velocity structure. More recently, Shen et al. (2025) proposed an incremental inversion strategy that gradually incorporates density and shear velocity model updates to obtain more accurate and realistic compressional velocity models using primarily P-wave reflection data.

This study focuses on seismic inversion for improved shear velocity modeling in 2D elastic isotropic media, using only pressure and converted S-to-P wave information recorded by hydrophones. It is assumed that the compressional velocity model is known and obtained from an inversion problem in advance. We employ wavefield reconstruction methods integrated with a multiple-point source scheme to recalculate forward wavefields during gradient computation efficiently. The numerical tool is built on top of the Devito framework (Luporini et al., 2018), and we evaluate the inversion through a conceptual model of the Brazilian pre-salt.

Methods

The governing equations of 2D elastic isotropic wavefield propagation in the velocity-stress formulation are the following:

$$\begin{aligned} \partial_t v_i &= 1/\rho \partial_j \sigma_{ij} + f_i \\ \partial_t \sigma_{ij} &= \left(\lambda \delta_{ij} \delta_{kl} + \mu\left(\delta_{il}\delta_{jk} + \delta_{ik}\delta_{jl}\right)\right)\left(\partial_l v_k - h_{kl}\right) \end{aligned} \quad (1)$$

Indices i and j assume values 1 and 2 and refer to the Cartesian coordinates x and z, respectively; v_i are the velocity components, σ_{ij} are the stress fields, ρ is the density, λ and μ are the Lamé parameters, δ_{ij} is Dirac's delta, and f_i and h_{ij} are the source injection terms. Although we deal with five wavefields, the velocity-stress formulation allows us to consider a multicomponent analysis natively. To simulate the 2D elastic wave propagation, we apply a 2D staggered-grid finite-difference scheme to Eq. 1 and Eq. 2, (Levander, 1988).

In the seismic inversion problem, our objective is to recover the shear wave velocity model that minimizes the mismatch between the observed seismic data, $\mathbf{d}_{obs}$, and the modelled data, $\mathbf{d}_{cal}$, across all source (S) and receiver (R) domains. Here, both $\mathbf{d}_{obs}$ and $\mathbf{d}_{cal}$ are hydrophone information and we quantify the mismatch using the L2-norm, defined as

$$\Psi = \frac{1}{2}\sum_{S,R}\int_0^T \|\mathbf{d}_{cal} - \mathbf{d}_{obs}\|^2 dt \tag{2}$$

The shear velocity gradient is defined by the sensibility of Eq. 2 concerning the shear velocity model, expressed in terms of the compressional V_p and shear V_s wave velocity models:

$$\frac{\partial \Psi}{\partial V_s} = \frac{2}{\rho V_s^3}\sum_{S,R}\int_0^t \left[\lambda_{xz}\partial_t\sigma_{xz} + \frac{1}{4}(\lambda_{xx} - \lambda_{zz})(\partial_t\sigma_{xx} - \partial_t\sigma_{zz}) - \frac{1}{4}\left(\frac{V_s^2}{V_p^2 - V_s^2}\right)^2 (\lambda_{xx} + \lambda_{zz})(\partial_t\sigma_{xx} + \partial_t\sigma_{zz})\right] dt \tag{3}$$

where λ_{ij} indicate the stress components of the adjoint wavefield.

Since we are only using hydrophone data, only indirect information of the elastic media will be observed in the loss function. To illustrate that, we highlight two types of events (see Figure 1):

1) P-wave conversion (P-P-P-S-P) from a upgoing S-wave, which was generated at the reflection point from a downgoing P-wave (P-P-P)
2) P-wave transmission (P-P-P-P-P), which will have the same travel time in acoustic and elastic media, but different amplitude due to the mode conversions.

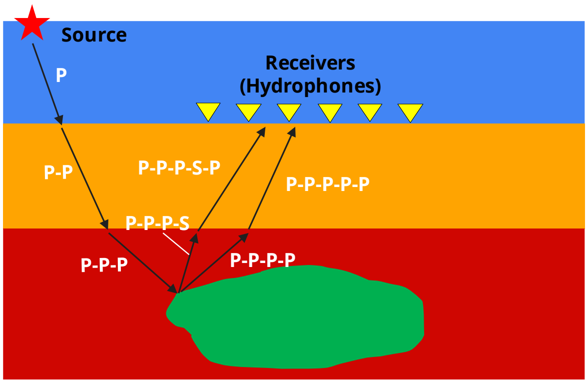

Figure 1: Indirect events of the elastic media observed by the hydrophone: P-wave conversion from a upgoing S-wave (P-P-P-S-P) and P-wave transmission (P-P-P-P-P).

We apply a preconditioning with a diagonal pseudo-Hessian matrix to incorporate amplitude compensation in the gradient. The diagonal components of this pseudo-Hessian matrix are,

$$I = \sqrt{\sum_S \int_0^t \left[\partial_t\sigma_{xz}\partial_t\sigma_{xz} + \frac{1}{4}(\partial_t\sigma_{xx} - \partial_t\sigma_{zz})(\partial_t\sigma_{xx} - \partial_t\sigma_{zz})\right] dt} \tag{4}$$

Since forward wavefield storage is highly memory demanding, we adopt the reconstruction scheme as shown in (Jaimes-Osorio et al., 2021).

Example

A synthetic model based on the Brazilian pre-salt is employed to estimate the shear velocity through the elastic full waveform inversion. The true and initial V_p and V_s models are indicated in Figure 2. Here, we use a solution obtained from a previous acoustic inversion as our initial V_p model. Our numerical experiments indicate that V_p should be solved first for the V_s inversion to properly proceed with the nonlinear problem convergence. The model grid size is (679, 421) with a spacing of 25 m. A perfectly matched layer (PML) is the absorbing boundary condition. The acquisition geometry consists of an ocean-bottom node configuration, as shown in Figure 2, with 183 sources (red stars) and 23 receivers (green triangles) with 75 m and 400 m spacing, respectively. We adopt the multiscale approach using the frequency band = {1, 2, 3} Hz. The true solution $\mathbf{d}_{obs}$ is the synthetic pressure seismogram obtained by solving full elastic wave propagation in true models. The L-BFGS method (Nocedal and Wright, 2006) is adopted as the nonlinear solver, and we define the maximum number of iterations as 20 for each frequency with a tolerance 10^{-8}.

Results

Figure 3(a) shows the results of the shear velocity inversion using a multiscale approach. Some crosstalk artifacts are present in the solution. Additionally, we observe acquisition geometry imprints in the V_s solution, mainly, for the results of 2 and 3 Hz. However, the main geological structures have been well reconstructed. Notably, the low-velocity zone at a depth of approximately 6.5 km is clearly recovered, as highlighted in Figure 3(b). Also, significant velocity contrasts associated with the salt body are well captured, particularly at its top and bottom boundaries are well recovered and in good agreement with true V_s model.

Conclusions

Our results suggest that shear velocity inversion may be achieved using only hydrophone data. Indirect information from S-waves—manifested through S-to-P conversions and amplitude variations in P-wave events—appear to carry sufficient information to reconstruct the main structures of the shear velocity model

Acknowledgments

This research was carried out in association with the R&D project registered as ANP nº 21950-1, “Caracterização e Modelagem de Caminhos Preferenciais de Fluxo nos Reservatórios do Pré-sal usando Ondas Cisalhantes”. (PUC Rio/Shell Brasil/ANP), sponsored by Shell Brasil Petróleo Ltda under the ANP R&D levy as “Compromisso de Investimentos com Pesquisa e Desenvolvimento”.'

References

Cho, Y., Pérez Solano, C., Kimbro, J., Yang, Y., Plessix, R. É., & Matson, K. (2022). Influence of shear velocity on elastic full-waveform inversion: Gulf of Mexico case study using multi-component OBN data. Geophysics, 87(5)

Jaimes-Osorio, L.E., Malcolm, A., Zheglova, P., Koene, E.F.M., Thomsen, H.R., 2021. Reduced memory implementation of a local elastic finite-difference solver. Geophysics 86, F25–F33.

Levander, A.R., 1988. Fourth-order finite-difference P-SV seismograms. Geophysics 53, 1425–

Luporini, F., Yount, C., Louboutin, M., Kukreja, N., Witte, P., Lange, M., Kelly, P., Herrmann, F., 2018. Devito automated high-performance finite differences for geophysical exploration.

Nocedal, J., Wright, S.J., 2006. Numerical Optimization, Second ed. Springer-Verlag, New York.

Sears, T.J., Singh, S.C., Barton, P.J., 2008. Elastic full waveform inversion of multi-component OBC seismic data. Geophysics. Prospect. 56, 843–862.

Shen, P., Albertin, U., Malcotti, H., Haataja, J., & Sekar, A. (2025). Feasibility of VP, VS , density inversion by elastic FWI. Leading Edge, May, 403–412.

Virieux, J., Operto, S., 2009. An overview of full-waveform inversion in exploration geophysics. Geophysics 74.

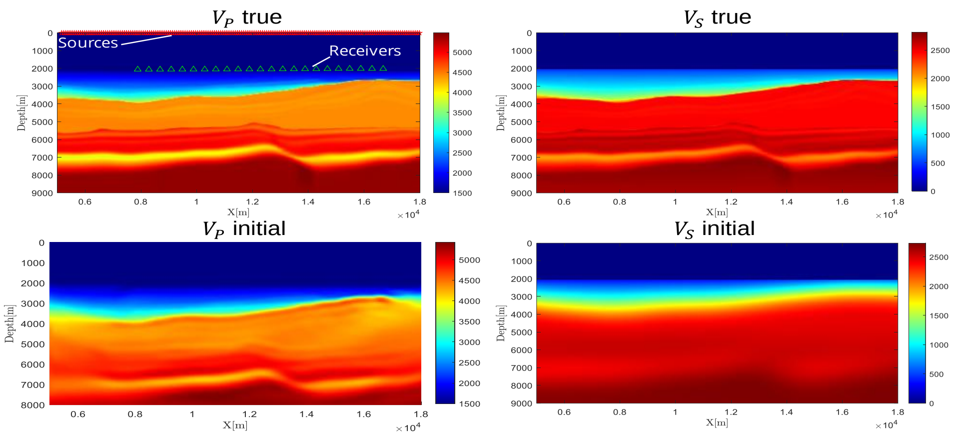

Figure 2: True and initial compressional and shear wave velocities models.

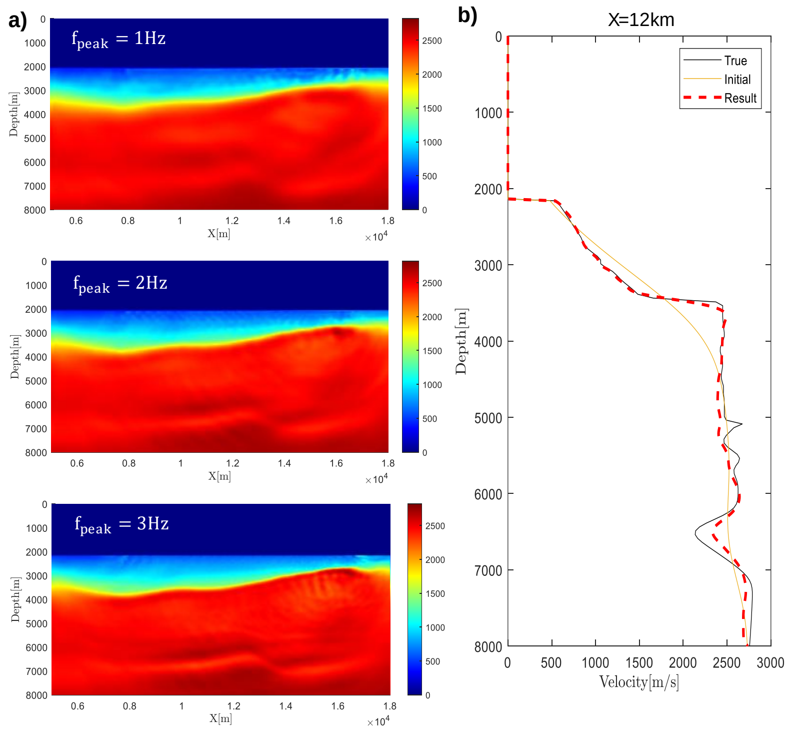

Figure 3: (a) the shear velocity wave inversion results using the multiscale approach. (b) Shear velocity profile of the true (black line), initial (yellow line), and recovered model (dashed red line) at x=12 km.